Journal of
Molluscan Studies

The Malacological Society of London

Journal of Molluscan Studies (2017) **83**: 304–315. doi:10.1093/mollus/eyx021
Advance Access publication date: 15 June 2017

Crystallographic texture analysis of Protobranchia (Mollusca: Bivalvia): interspecific variations, homology and shell microstructural evolution

Kei Sato[1,2], Antonio G. Checa[3], Alejandro B. Rodríguez-Navarro[4] and Takenori Sasaki[2]

[1]*Department of Geology and Mineralogy, Kyoto University, 340 Science Department I, Kitashirakawaoiwake-cho, Sakyo-ku, Kyoto-shi 606-8502, Japan;*
[2]*The University Museum, University of Tokyo, 7-3-1 Hongo, Bunkyo-ku, Tokyo 110-0033, Japan;*
[3]*Departamento de Estratigrafía y Paleontología, Universidad de Granada, 18071 Granada, Spain; and*
[4]*Departamento de Mineralogía y Petrología, Universidad de Granada, 18071 Granada, Spain*

Correspondence: K. Sato; e-mail: keisato@kueps.kyoto-u.ac.jp

(Received 28 December 2016; editorial decision 17 April 2017)

ABSTRACT

To achieve a better understanding of the formation and evolutionary history of molluscan shell microstructures, we analysed crystallographic textures of shell microstructures of selected species of Protobranchia, the most ancient group of Bivalvia. Our dataset covers four of the five protobranch superfamilies. Shell layers of five species of Nuculoidea, four species of Solemyida and seven species of Nuculanoidea were analysed and classified according to their textural crystallographic patterns into six different types. Our investigation revealed that some microstructures (e.g. the radially elongate simple prismatic structure) have structure-specific textural patterns, while other microstructures (e.g. the homogeneous structure) show taxon-specific differences despite morphological similarities. The former result means that each microstructure accurately reflects a unique crystallographic structure; the inconsistency in the latter, however, calls into question the homologies among morphologically defined microstructures. In comparison with the latest molecular phylogenetic trees, our data showed that crystallographic textures are phylogenetically constrained within Protobranchia. Each nuculoidean species had two to three distinct textural patterns, and one or two similar textural patterns were recognized within each species of Solemyida and Nuculanoidea. In general, closely related species had similar crystallographic textural patterns regardless of differences in shell microstructures.

INTRODUCTION

Molluscan shells are some of the most intensively studied biomineral aggregates. They consist of calcium carbonate and minor amounts of organic matter. The calcium carbonate in shells usually takes the form of aragonite and/or calcite, and rarely vaterite (e.g. Spann, Harper & Aldridge, 2010). The mineral phase, nucleation, shape and orientation of shell crystals in molluscs are controlled by crystallographic and biological processes. As a result, crystals are organized in recurrent structural arrangements called shell microstructures. Molluscan shells are secreted incrementally by the cells of the mantle epithelium, which are virtually in contact with the inner surface of the shell. The shells generally contain several superimposed layers (Taylor, Kennedy & Hall, 1969), which may differ in mineralogical composition and/or microstructure (e.g. crystal orientation; MacClintock, 1967). The structural organization of molluscan shells has been well studied over several decades and its diversity has been widely recognized (e.g. Bøggild, 1930; Taylor, Kennedy & Hall, 1969; Taylor, Kennedy & Hall, 1973; Carter, 1990). In an extensive review of molluscan shell microstructures, Carter (1990) categorized molluscan shell microstructures into 42 morphotypes. This variety in molluscs is well above that found in other animal phyla or subphyla (e.g. brachiopods, corals or vertebrates; Carter, 1990). It is, therefore, intriguing how molluscan shell microstructures are determined and why they are so variable.

With regard to the variability of molluscan shell microstructures, it is widely accepted that shell microstructures are phylogenetically constrained. Numerous studies have described shell microstructural compositions and confirmed similarities between phylogenetically close taxa in diverse groups of molluscs (Veneridae: Uozumi & Suzuki, 1981; Littorinidae: Taylor & Reid, 1990; Cardiidae: Schneider & Carter, 2001; Patellogastropoda: Fuchigami & Sasaki, 2005; Mytilidae: Génio *et al.*, 2012). Even the shell microstructures of fossil molluscs have been described for a variety of taxa (e.g. Carter, 1990, 2001; Hedegaard, Lindberg & Bandel, 1997; Kouchinsky, 2000; Schneider & Carter, 2001; Feng & Sun, 2003; Vendrasco, Checa & Kouchinsky, 2011). Further studies characterizing variations in shell microstructure among clades are expected to provide a better understanding of both the evolutionary history and the biomineralization mechanisms of molluscs.

Shell microstructures are mostly characterized based on observations by qualitative methods: light microscopy, scanning electron microscopy (SEM) and transmission electron microscopy. However,

Table 1. List of the specimens analysed in this study. All localities are in Japan.

Classification	Species	Sample number	Latitude	Longitude	Depth (m)	Locality
Order Nuculanida, Superfamily Nuculoidea						
Nuculidae	*Acila vigilia* Schenck, 1936	RM32595	41°05.46′N–41°07.15′N	141°36.83′E–141°36.17′E	537.1–560	Off Nakayamasaki
	Acila insignis (Gould, 1861)	RM32230	39°20.28′N	141°54.56′E	15.2	Otsuchi Bay
	Sinonucula cyrenoides (Kuroda, 1929)	RM32596	38°17.06′N–38°16.94′N	141°41.05′E–141°40.94′E	147.1–147.7	Off Kinkasan
	Ennucula niponica (Smith, 1885)	RM32597	33°34.6′N	135°00.0′E	556.53	Off Wakayama
	E. niponica (Smith, 1885)	RM32598	28°33.89′N–28°32.96′N	127°02.62′E–127°02.20′E	610–611	Off Amami-Ohshima
	Nucula sp.	RM32599	33°31.8′N	134°59.3′E	998.92	Off Wakayama
Order Solemyida, Superfamily Solemyoidae						
Solemyidae	*Acharax japonica* (Dunker, 1882)	RM32600	34°40.04′N	138°56.08′E	0.5	Shimoda Marine Resarch Centre
	Acharax johnsoni (Dall, 1891)	RM32601	28°33.89′N–28°32.96′N	127°02.62′E–127°02.20′E	610–611	Off Amami-Ohshima
	Solemya pusilla Gould, 1861	RM32602	–	–	approx. 5	Off Notojima, Ishikawa Prefecture
Order Solemyida, Superfamily Manzanelloidea						
Nucinellidae	*Huxleyia sulcata* A. Adams, 1860	RM32603	35°07.19′N–35°06.86′N	139°34.10′E–139°33.75′E	210–345	Off Misaki
Superfamily Nuculanoidae						
Nuculanidae	*Nuculana tanseimaruae* Tsuchida & Okutani, 1985	RM32604	33°34.6′N	135°00.0′E	556.53	Off Wakayama
	N. tanseimaruae Tsuchida & Okutani, 1985	RM32605	32°09.07′N–32°09.02′N	128°59.03′E–129°00.45′E	508–514	Okikasayama Bank
	Saccella gordonis (Yokoyama, 1920)	RM32606	35°10.31′N–35°10.24′N	139°34.81′E–139°34.74′E	85.5–87.7	Off Misaki
Malletiidae	*Malletia takaii* Okutani, 1968	RM32607	38°29.83′N–38°29.77′N	143°06.98′E–143°04.66′E	2307	Off Onagawa
Tindariidae	*Tindaria soyoae* Habe, 1953	RM32608	28°32.27′N–28°34.15′N	127°02.28′E–127°02.53′E	606–610	Off Amami-Ohshima
Neilonellidae	*Neilonella soyoae* Habe, 1958	RM32609	33°34.6′N	135°00.0′E	556.53	Off Wakayama
Yoldiidae	*Yoldia johanni* Dall, 1925	RM32262	43°06.68′N–43°06.61′N	145°45.67′E–145°45.40′E	94–95	Off Nemuro Peninsula
	Yoldia notabilis Yokoyama, 1922	RM32610	39°20.22′N	141°54.21′E	10	Otsuchi Bay

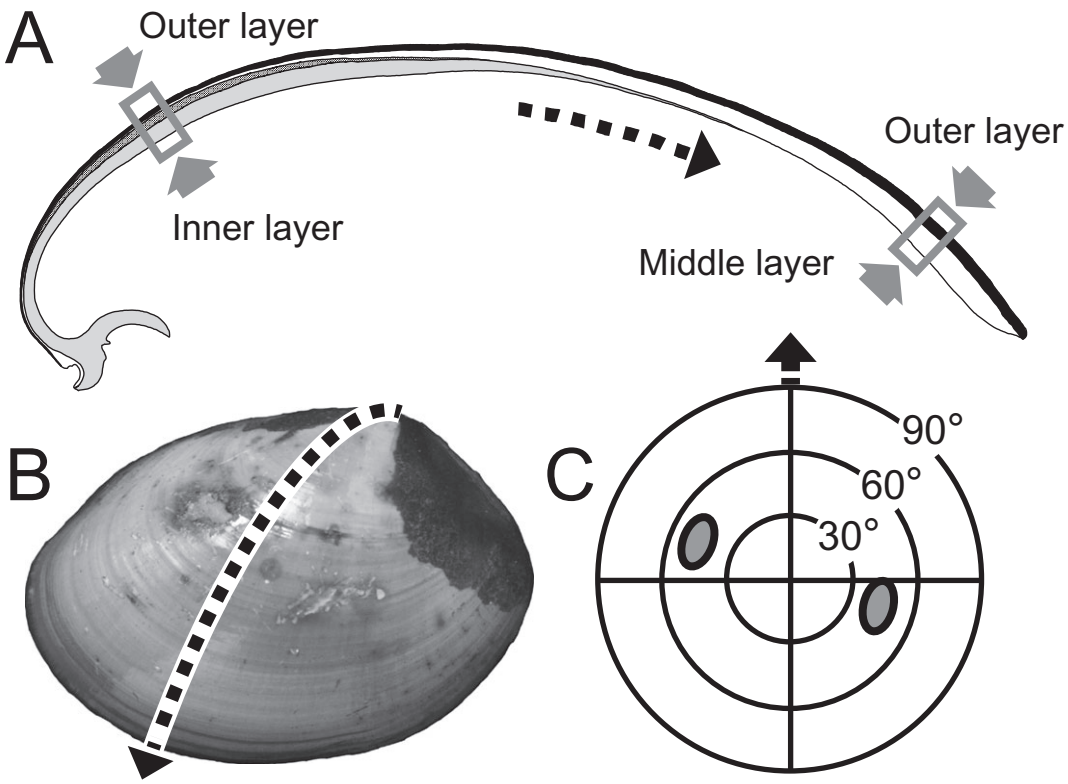

Figure 1. A. Diagram of radial section of *Ennucula niponica*, showing distribution of outer, middle, myostracum and inner layers. Dashed arrow indicates direction of growth. Crystallographic textures of each layer were analysed at outer and inner surfaces on small chips from dorsal and ventral sides of shell. Note that middle layer is exposed to inner shell surface at ventral side of shell and, on the other hand, inner layer covers inner shell surface at dorsal side. **B.** External shell morphology of *E. niponica*. Dashed arrow coincides with the sectioned plane shown in **A**. **C.** Schematic diagram of an example of an XRD pole figure. Arrow indicates growth direction of shell.

Table 2. Characterization of the six types of crystallographic textures defined in this study.

Defined crystallographic texture type	Direction 102	Direction 002
Type A	Scattered distribution or ring-like pattern	Deeply reclined (at least 30°)
Type B	Two or three peaks showing parallel to linear patterns	Two distinct peaks; deeply reclined (at least 30°) and nearly vertical (up to 30°)
Type C	Weakly clustered to girdle-like pattern	Nearly vertical (up to 30°)
Type D	Single crystal-like	Nearly vertical (up to 30°)
Type E	Double twin-like	Nearly vertical (up to 30°)
Type F	Scattered distribution	Zonate distribution (FWHM at least 30°), nearly vertical (up to 30°)

characterizing the crystallographic textures is also important to allow the quantitative evaluation of ordered microstructures and to investigate the mechanisms responsible for their development (Checa & Rodríguez-Navarro, 2005). Furthermore, several studies have reported that the crystallographic textures of molluscan shell microstructures are phylogenetically constrained (e.g. Chateigner, Hedegaard & Wenk, 2000; Álvarez-Lloret, Rodriguez-Navarro & Checa, 2008; Frýda *et al.*, 2010). One example is the *a*- and *b*-axis directions of nacre, one of the most studied microstructures. Chateigner *et al.* (2000) and Álvarez-Lloret *et al.* (2008) considered that in bivalves, contrary to gastropods, these axes are co-oriented. In addition, Frýda *et al.* (2010) recognized that the alignment of *a*- and *b*-axes of nacre of bivalves differs at the level of order to genus and that they show a tendency to be well-ordered in more derived bivalve groups.

For protobranch bivalves, crystallographic texture analyses are limited, although morphological descriptions of microstructures have been performed (Sato *et al.*, 2013; Sato & Sasaki, 2015). In these studies, a diversity greater than that of the previously known shell microstructures has been revealed. For instance, Sato *et al.* (2013) subdivided the unique microstructure of Solemyoidea, the radially elongate simple prismatic structure, into three types. Also, five types of the outer prismatic layer were recognized in Nuculoidea (Sato & Sasaki, 2015). Protobranchia is widely regarded as the most basal group of bivalves (e.g. Zardus, 2002); hence, it is a key taxon for understanding the origin and evolution of shell microstructures in Bivalvia. Protobranchs have not changed their large-scale morphology drastically over time and their range of variation is relatively limited (Zardus, 2002). Therefore, the characterization of their shell microstructures both by morphological descriptions and crystallographic texture analyses will provide information about phylogenetic groupings within the Protobranchia.

The crystallographic textures of shell microstructures are adequately described using X-ray pole figures displaying the

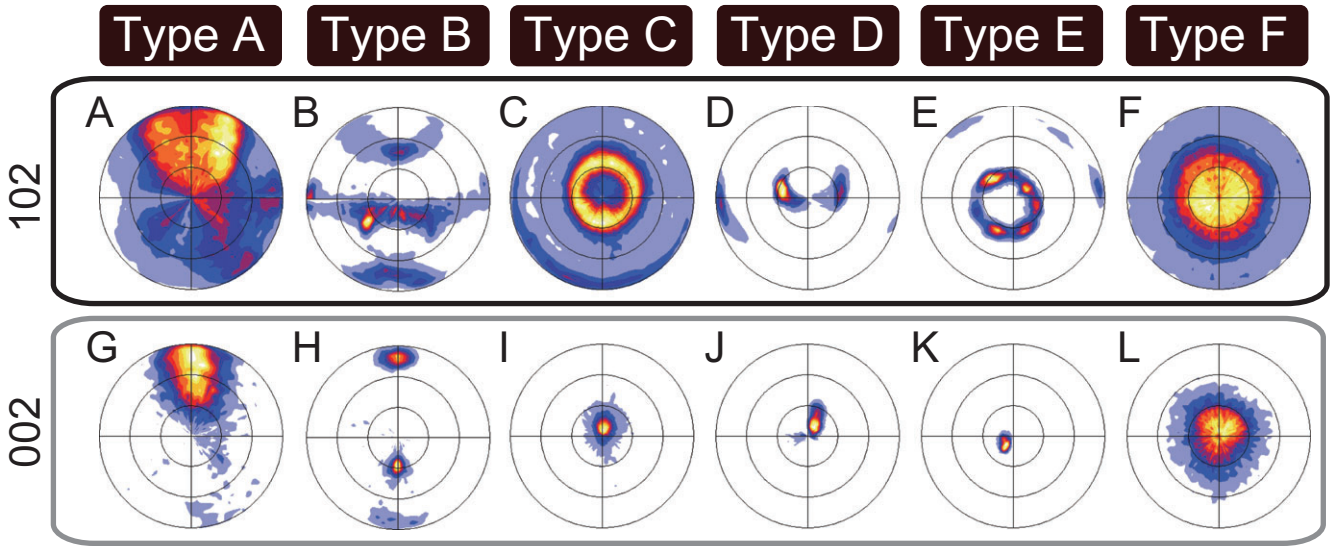

Figure 2. Pattern diagrams of crystallographic textures found in this study. We classified the pole figures into six different crystallographic patterns (see text).

distribution of specific crystallographic directions, or poles, in relation to the sample surface. Here, we analysed crystallographic textures of shell microstructures of protobranchs and categorized their pole figures to test homologies across various higher taxa, using the set of species described morphologically by Sato & Sasaki (2015).

MATERIAL AND METHODS

Material

In total, 18 specimens belonging to 16 species of Protobranchia from Japanese waters were investigated in this study (Table 1). Their higher classification is based on current systematics (Bouchet *et al.*, 2010; Huber, 2010; Coan & Valentich-Scott, 2012; WoRMS, 2016). Two specimens of both *Ennucula niponica* and *Nuculana tanseimaruae* from different localities were used to check for intraspecific variation in crystallographic textures.

Scanning electron microscopy

Polished surfaces of the shells of these species were observed with an SEM (Keyence-VE8800). Specimens were embedded in epoxy resin (S-31, Devcon Corp.) prior to cutting, immersed in sodium hypochlorite for 15 min, and etched with 0.2% HCl for 1 min. After cleaning with an ultrasonic cleaner, the samples were coated with osmium using an osmium coater (Vacuum Device HPC-15W) for observations by SEM. The terminology used for shell microstructures was based on Carter (1990) and Carter *et al.* (2012).

X-ray diffraction (XRD)

Pole figures were measured from the variation of intensity of a given *hkl* reflection for any possible orientation of the sample. Prior to XRD, all samples were cut into small chips (up to *c.* 5 mm in diameter) using a hand cutter. Small chips were cut from areas near the dorsal and ventral margins of the shells and the outer, middle and inner layers; they were then exposed to X-rays (Fig. 1). Samples were measured using an X-ray single diffractometer (SMART APEX II, Bruker, located at Chiba University) with the following working conditions: Mo Ka radiation 50 kV and 30 mA, collimator size 0.5 mm in diameter. The shell samples were mounted on a goniometer head with the target surface perpendicular to the ϕ–rotation axis. The ϕ axis was rotated by 180° or 360°, with diffraction patterns being recorded every 5°, giving a total of 36 or 72 frames for each analysis. The ω and 2θ axes were set at 10° and 20°, respectively. As a result, the orientation distribution was determined for thousands of crystallites in an area that was only around 1–3 mm in diameter. Pole densities for strong aragonite reflections (102 and 002) were calculated and displayed using the XRD2DScan software v. 4.1.1 (Rodriguez-Navarro, 2006; http://www.ugr.es/~anava/xrd2dscan.htm). Pole figures display intensity variations of a given *hkl* reflection (102, 002) as a function of the sample orientation. The upper side of all of the generated pole figures coincides with the growth direction of each shell. The angular width of the maxima displayed in the pole figures was calculated along the ϕ and χ angles, thus representing the spread of crystal orientations for a particular sample. If the analysed polycrystalline materials are composed of aligned crystals, the pole figures show sharp maxima, while materials consisting of disordered crystals show a scattered distribution in their pole. In general terms, {102} poles provide indications of the *a*-axis distributions and we can interpret *c*-axis distributions from {002} poles.

RESULTS

The observed crystallographic texture patterns were classified into six groups based on the qualitative and quantitative analyses of pole figures. Our characterization and definition of textural groups are summarized in Table 2 and Figure 2. Most shell microstructural compositions we analysed had already been described by Sato *et al.* (2013) and Sato & Sasaki (2015). However, we provide the first descriptions of the shell microstructures of *Sinonucula cyrenoides* and *Acila vigilia*. The shell microstructures of the protobranchs analysed and their attribution to textural groups are shown in Table 3 (see also Supplementary Material Fig. S1; Sato *et al.*, 2013; Sato & Sasaki, 2015), along with the descriptions of their crystallographic patterns. Shell microstructures and crystallographic textures did not exhibit a simple one-to-one correspondence; their complex relationship is described below.

Nuculidae

Our SEM observation revealed that both *A. vigilia* and *S. cyrenoides* shells commonly had an irregular nondenticular composite prismatic outer layer, a columnar nacreous middle layer and

Table 3. Results of the textural investigations. Abbreviations of shell microstructures as in Figure 4.

Specimens	Shell layers	Microstructure	Type of textural pattern	maximum FWHM of {002} pole	Inclined angle of {002} pole at the strongest intensity	Qualitative diagnosis
Acila vigilia	Outer (dorsal part)	INDCP	Type A	*c*. 50°	>40°	–
	Outer (ventral part)		Type A	*c*. 50°	>60°	–
	Middle	Columnar N	Type C	*c*. 25°	<10°	–
	Inner	Sheet N	Type C	*c*. 30°	<17°	–
Acila insignis	Outer	IFP	Type A	*c*. 40°	>60°	–
	Middle	Columnar N	Type C	*c*. 15°	<15°	Showing a tendency to develop a dyad symmetry pattern in the {102} pole
	Inner	Sheet N	Type C	*c*. 10°	<10°	Showing a tendency to develop a dyad symmetry pattern in the {102} pole
Sinonucula cyrenoides	Outer (dorsal part)	INDCP	Type C	*c*. 35°	*c*. 20°	–
	Outer (ventral part)		Type A	*c*. 40°	>50°	–
	Middle	Columnar N	Type D	*c*. 21°	<10°	–
	Inner	Sheet N	Type C	*c*. 20°	<10°	–
Ennucula niponica off Wakayama	Outer (dorsal part)	NDCP	Type C	*c*. 20°	<10°	–
	Outer (ventral part)			*c*. 20°	*c*. 25°	–
	Middle	Columnar N	Type D	*c*. 20°	<10°	–
	Inner	Sheet N	Type C	*c*. 30°	<10°	Showing weak tendency to develop a six-maxima pattern in the {102} pole
E. niponica off Amami-Ohshima	Outer (dorsal part)	NDCP	Type C	*c*. 40°	<10°	–
	Outer (ventral part)			*c*. 25°	*c*. 20°	–
	Middle	Columnar N	Type C	*c*. 17°	<10°	Showing a tendency to develop a dyad symmetry pattern in the {102} pole
	Inner	Sheet N	Type E	*c*. 10°	*c*. 5°	–
Nucula sp.	Outer	DCP	Type B	*c*. 16°	>70°	–
	Middle	Columnar N	Type D	*c*. 24°	<30°	–
	Inner	Sheet N	Type E	*c*. 20°	<30°	A six-maxima pattern in the {102} pole is relatively unclear
Acharax japonica	Outer	RESP Type C	Type C	*c*. 35°	<10°	Showing a tendency to develop clusters in the {102} pole
	Inner	Laminar	Type C	*c*. 14°	<10°	
Acharax johnsoni	Outer	Reticulate	Type F	*c*. 30°	*c*. 10°	Showing a weak tendency of clustering
	Inner	cone CCL	Type F	*c*. 40°	<30°	Showing a weak tendency of clustering
Solemya pusilla	Outer	RESP Type B	Type C	*c*. 20°	*c*. 10°	Showing a tendency to develop a dyad symmetry pattern in the {102} pole
	Inner	Hom.	Type C	*c*. 30°	<10°	
Huxleyia sulcata	Outer	Hom.	Type F	*c*. 40°	<10°	–
	Inner	Hom.	–	–	–	–
Nuculana tanseimaruae off Wakayama	Outer	Fibrous P	Type C	*c*. 21°	*c*. 18°	–
	Middle to inner	Hom.	Type C	*c*. 10°	<10°	The {102] poles show ain irregularly clustered pattern
Nuculana tanseimaruae off Amami-Ohshima	Outer	Fibrous P	Type C	*c*. 20°	*c*. 15°	–
	Middle to inner	Hom.	Type C	*c*. 10°	<10°	The {102] poles show an irregularly clustered pattern
Saccella gordonis	Outer	Fibrous P	Type F	*c*. 35°	*c*. 30°	–
	Middle to inner	Hom., fine CCL	Type E	*c*. 25°	<10°	–

Malletia takaii	Outer to middle	Hom.	Type F	c. 60°	–	–	–
	Inner	Fine CCL	Type C	c. 20°	<10°	–	–
Tindaria soyoae	Outer	Hom.	Type F	c. 45°	c. 20°	–	–
	Inner	Hom.	Type C	c. 25°	<10°	–	–
Neilonella soyoae	Outer	Fibrous P	Type F	c. 40°	c. 30°	–	–
	Middle to inner	Hom.	Type C	c. 17°	<10°	–	–
Yoldia johanni	Outer (dorsal part)	Hom.	Type C	c. 25°	<10°	–	–
	Outer (ventral part)	Hom.		c. 20°	<10°	–	–
	Middle	Hom.	Type C	c. 13°	<10°	–	–
	Inner	Fine CCL	Type C	c. 11°	<10°	–	–
Yoldia notabilis	Outer	Hom.	Type C	c. 20°	<10°	–	–
	Middle	Hom.	Type C	c. 10°	<10°	–	–
	Inner	Fine CCL	Type C	c. 16°	<10°	–	–

a sheet nacreous inner layer (Fig. 3). The crystallographic textures of the five nuculid species are shown in Supplementary Material Figs S2 and S3. In the larger species (i.e. *A. vigilia*, *Ennucula niponica*, and *S. cyrenoides*), the crystallographic textures of their outer layers were determined at both the ventral and the dorsal sides.

Species of the family Nuculidae commonly have prismatic structures in their outer shell layers, with considerable interspecific morphological variation (see Sato & Sasaki, 2015). Among the examined species, *E. niponica* has a nondenticular composite prismatic structure, *A. insignis* has an irregular fibrous prismatic structure and *Nucula* sp. has a denticular composite structure. The variation in the crystallographic textures of the outer layers of nuculid species was discernible at the ventral side of each shell (i.e. the area where the outer layer thickens). Although they do not share the same shell microstructures in their outer layers and differ in the presence or absence of shell sculpture, the crystallographic textures of *A. insignis*, *A. vigilia* and *S. cyrenoides* (Supplementary Material Fig. S2B, F, I, L and S3B, F) were similar, showing deeply slanting {002} pole maxima and ring-like patterns in the {102} pole figures (type A). The crystallographic texture of the outer prismatic layer of *N.* sp. (Supplementary Material Fig. S2O, R) differed slightly from that of the above species in that the crystals in the outer layer were better aligned and two different maxima on the {002} poles were recognized, with one of the them being likewise deeply reclined {002}. One region was deeply slanting (almost 90°) and the other was tilted by *c.* 30° (type B). The denticular composite prismatic structure of the outer layer of *N.* sp. consisted of acicular crystals spreading ventrally in a fan-like manner; acicular crystals on the exterior side of the outer layer were nearly perpendicular to the outer shell surface and those on the interior side were almost horizontal (see Sato & Sasaki, 2015: figs 112–117). Thus, the crystallographic pattern recognized in the outer layer of *N.* sp. is presumably related to this crystal distribution. The crystallographic textures of *E. niponica* (Supplementary Material Fig. S3I–X) showed weakly slanting {002} poles (around 30°) and a ring-like pattern, while the {102} poles tended to cluster (type C).

The middle and inner layers of the family Nuculidae are commonly composed of nacreous structures, but differences in the stacking pattern of nacre tablets are obvious between the middle and inner layers in most nuculids (Sato & Sasaki, 2015). The nuculid species we examined commonly have columnar nacre in their middle layers and sheet nacre in their inner layers. While the *c*-axes of the nacreous structures were nearly perpendicular to the shell surfaces in all examined nuculids, the distribution of their {102} poles was variable. Dyad symmetry patterns, which imply a single crystal-like texture (type D), were found for the {102} poles in the middle layers of *N.* sp. (Supplementary Material Fig. S2P), *S. cyrenoides* (Supplementary Material Fig. S3C) and *E. niponica* (a specimen from off Wakayama; Supplementary Material Fig. S3S). Weakly clustered girdle-like patterns (type C) were recognized in the middle layers of *E. niponica* (a specimen from off Amami-Ohshima; Supplementary Material Fig. S3K) and *A. insignis* (Supplementary Material Fig. S2J). The middle layer of *A. vigilia* showed a ring-like pattern (type C) in the {102} pole, indicative of a fibrous texture (Supplementary Material Fig. S2C). The inner-layer sheet nacreous structure in the two *Acila* species (Supplementary Material Fig. S2D, K) had a crystallographic texture similar to that of their middle-layer columnar nacreous structure. However, the middle- and inner-layer nacreous structures of the other nuculids had different shell textures, with the {102} poles of their inner nacreous layers more widely scattered than in their middle nacreous structures. For instance, in the two specimens of *E. niponica*, the {102} poles in the inner layers showed six maxima (type E) (Supplementary Material Fig. S3L, T). In addition, a similar pattern was recognized, but was not as distinct, in *N.* sp. (Supplementary Material Fig. S2Q). The six maxima can be interpreted as products of the high incidence of double (polycyclic)

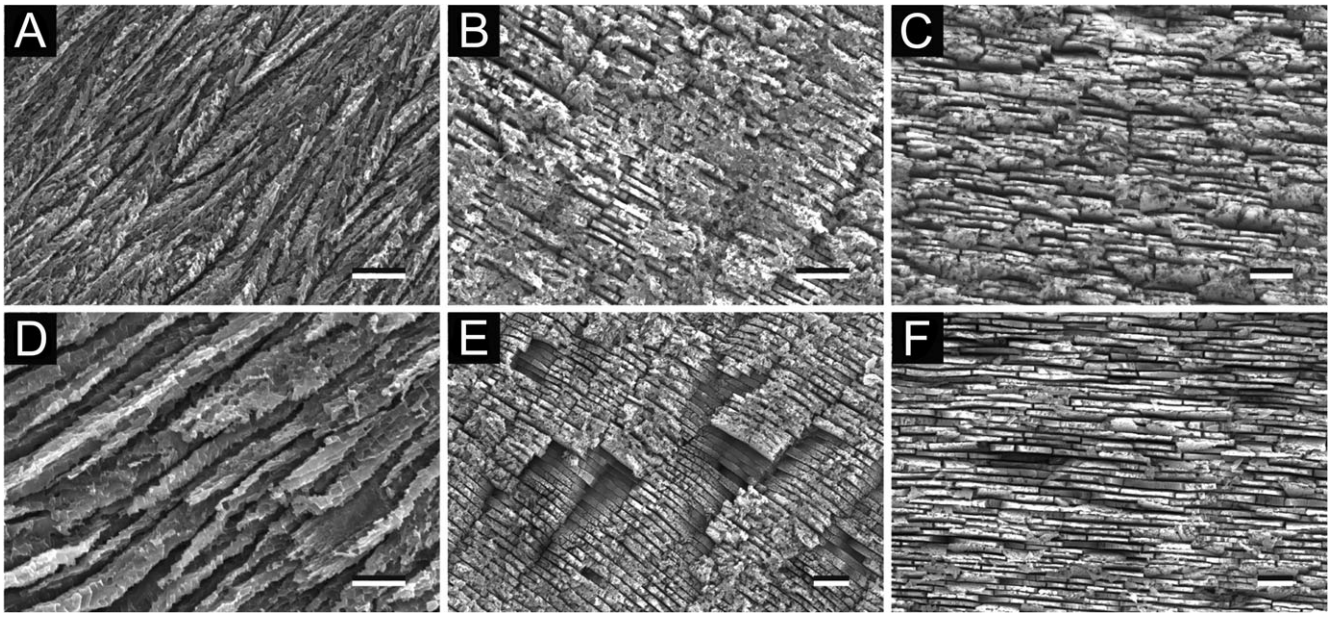

Figure 3. Scanning electron micrographs of *Acila vigilia* (**A–C**) and *Sinonucula cyrenoides* (**D–F**) microstructures. All images show radial sections of each shell and growth direction is toward the left in all cases. **A.** Irregular nondenticular composite prismatic structure of outer layer. **B.** Columnar nacreous structure of middle layer. **C.** Sheet nacreous structure of inner layer. **D.** Irregular nondenticular composite prismatic structure of outer layer. **E.** Columnar nacreous structure of middle layer. **F.** Sheet nacreous structure of inner layer. Scale bars = 5 μm.

twinning (Chateigner *et al.*, 2000; Frýda *et al.*, 2010). The {102} poles of the inner-layer nacre of *S. cyrenoides* showed a nearly ring-like pattern (type C; Supplementary Material Fig. S3D), while its middle nacreous layer showed a dyad symmetry pattern.

Solemyida

The Solemyidae (superfamily Solemyoidea) exhibit considerable variation in shell microstructures (see Sato *et al.*, 2013); however, their crystallographic textures were found to be uniform (Supplementary Material Fig. S4). *Acharax johnsoni* possesses a reticulate structure in the outer layer and cone complex crossed lamellar (cone CCL) structure in the inner layer. Nevertheless, they had irregular shapes and only barely clustered, circular distributions (type F) were commonly found in the {102} pole figures in both layers (Supplementary Material Fig. S4A–D). The outer layers of *A. japonica* and *Solemya pusilla* have a common radially elongate simple prismatic structure. On the other hand, their inner layers differ from each other: *A. japonica* has a laminar and *S. pusilla* a homogeneous structure. Nevertheless, the main crystallographic directions of the two layers in both species are similar (type C crystallographic textures; Supplementary Material Fig. S4E–L).

The shell of *Huxleyia sulcata*, which belongs to Manzanelloidea, has an entirely homogeneous structure. Its crystallographic texture showed a circular distribution of the {102} pole (type F; Supplementary Material Fig. S4M).

Nuculanoidea

In contrast to the above-mentioned taxa, the shell microstructures of the superfamily Nuculanoidea are generally uncomplicated and a homogeneous structure was observed in all studied species. On the other hand, the crystallographic textures were not uniform, even for the same microstructures (Supplementary Material Fig. S5, 6). Two species of Nuculanidae, *Nuculana tanseimaruae* and *Saccella gordonis*, and one species of Neilonellidae, *Neilonella soyoae*, have fibrous prismatic structures in their outer layer. However, their crystallographic textures were not the same. While the fibrous prismatic structures of two *N. tanseimaruae* specimens showed a girdle-like distribution of their {102} poles and weakly reclined {002} poles (around 15°) (type C) (Supplementary Material Fig. S5E, I), those of *S. gordonis* and *N. soyoae* showed much more scattered {102} and {002} poles (type F; Supplementary Material Fig. S5A, B, U, V). Similarly, the homogeneous structure in each species was defined by three distinct crystallographic textural patterns. Type F crystallographic textures were recognized in the outer layers of *Malletia takaii* and *Tindaria soyoae* (Supplementary Material Fig. S5M, N, Q, R). Meanwhile, the outer layers of two *Yoldia* species (Supplementary Material Fig. S6A, B, E, F) and the inner layers of *T. soyoae* (Supplementary Material Fig. S5S, T) and two specimens of *N. tanseimaruae* (Supplementary Material Fig. S5G, K) showed type C crystallographic textures. *Saccella gordonis*, exceptionally, showed the type E crystallographic pattern (Supplementary Material Fig. S5C, D). Fine complex crossed-lamellar structures (fine CCL) in the inner layers of *T. soyoae*, *N. soyoae* and two *Yoldia* species (Supplementary Material Fig. S5S, T, W, X; 8D, H, K, N) showed type C patterns.

DISCUSSION

Substantial diversity in crystallographic textures has been documented in various molluscan shells and we present detailed data with broader taxonomic sampling in protobranch bivalves. Chateigner *et al.* (2000) characterized the crystallographic textures of shell microstructures in 50 molluscan species using X-ray diffractometry. They found that the nacreous structures of bivalves and cephalopods had six maxima in the *a*-axis direction (equivalent to our type E pattern) and that those of gastropods and monoplacophorans had a ring-like pattern in the same direction (our type C). After examining the nacre of 12 species from the families Nuculoidea, Ostreida, Mytilida, Unionida and Trigoniida, they concluded that all bivalves had the same textural pattern. On the other hand, Frýda *et al.* (2010) conducted an electron backscatter diffraction analysis on the crystallographic textures of nacreous structures within four bivalve taxa: Nuculidae, Mytilida, Ostreida and Unionida. They concluded that unordered nacre (ring-like pattern; our type C) was found in basal groups of bivalves and that ordered nacre (our types D and E) occurred in more derived

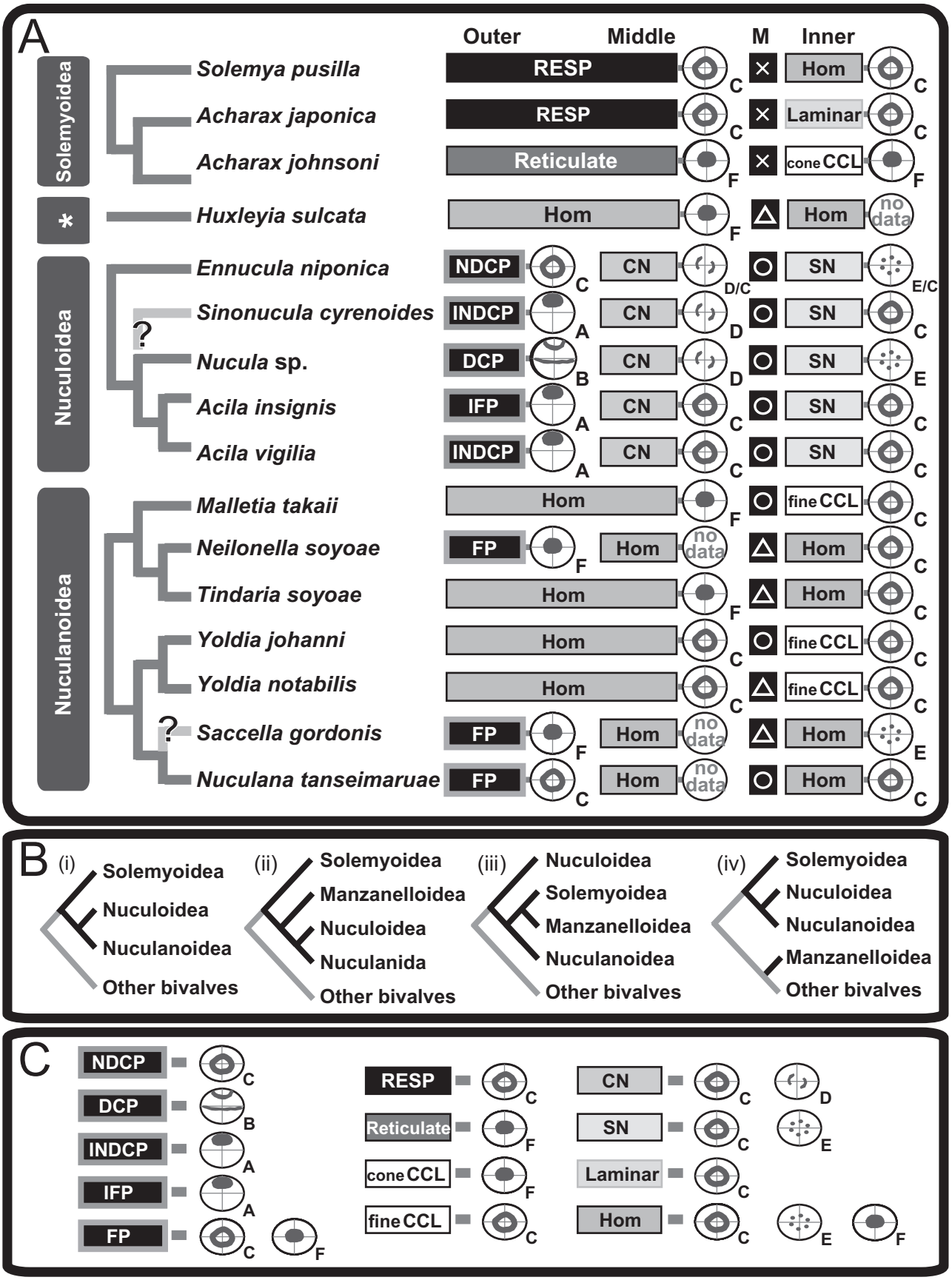

Figure 4. A. Schematic illustration showing phylogenetic relationships between the examined species, on the basis of phylogenetic tree by Sharma *et al.* (2013), shell microstructural assemblages (data from Sato & Sasaki, 2015 and this study) and pattern diagrams of crystallographic patterns of the {102}

taxa. In addition, they found a variety of ordered and disordered nacreous structures within a family or genus, or even within different shell layers of the same species. As to other microstructures, Almagro *et al.* (2016) reported remarkable crystallographic diversity in the crossed lamellar structures among bivalve and gastropod shells. In line with these reports, our study shows that crystallographic textures are variable in aragonitic prismatic, fine CCL and homogeneous structures among protobranchs.

Our crystallographic data on two specimens each of *Ennucula niponica* and *Nuculana tanseimaruae* from two different localities imply that the crystallographic textures in these shells show little intraspecific variation. Several studies have reported that crystal forms, size and orientation of molluscan shells are affected by some environmental factors (e.g. water temperature, Wada (1972), Olson & Gilbert, 2012a; Olson *et al.*, 2012b; pH, Hahn *et al.*, 2014). Thus, one possibile explanation for the intraspecific variation in these species could be related to physical factors. By comparing the crystallographic textures, we found that, as expected, interspecific variation in crystallographic textures was more significant than intraspecific variation and that, in some cases, similarity in crystallographic aspects can be established between closely related taxa (Fig. 4). These results strongly imply that crystallographic textures are phylogenetically constrained, as described below.

Phylogenetic constraint of crystallographic textures

Nuculoidea: The textural patterns of nuculoidean outer layers seem to provide robust signals for their phylogenetic groupings. For example, two *Acila* species commonly showed type A patterns in their outer layers, even though they are seemingly composed of different microstructures. *Acila vigilia* has an irregular nondenticular composite prismatic structure in the outer layers, while the outer layer of *A. insignis* shows an irregular fibrous prismatic structure. These microstructures differ in their first-order structure, but share long acicular crystals (high length/width ratio) as second-order structural units (see definition by Sato & Sasaki, 2015). We therefore consider that their microstructural differences, as defined by the first-order microstructures, are not significant in crystallographic terms. The crystallographic texture of the outer layer of *N.* sp. showed a pattern similar to that of *Acila* species (type B). *Nucula* and *Acila* were sister groups in the molecular phylogenetic analysis by Sharma *et al.* (2013), while *Ennucula* species occupy a position that is basal to other nuculids in their phylogenetic tree. This topology seems to be consistent with the differences we found in their crystallographic textures: only *E. niponica* had an exceptional pattern (type C). Unlike the other nuculids, the crystallographic *a*-axis does not follow the long axes of acicular crystals composing the outer layer of *E. niponica* (see Sato & Sasaki, 2015: fig. 79), thus suggesting an unusual mechanism of crystal formation. While the molecular phylogenetic position of *Sinonucula* is still unknown, *S. cyrenoides* may be close to *Acila* or *Nucula* based on the type A textural pattern of its outer layer.

Solemyida: The monophyly of Solemyida is controversial in current studies on molecular phylogeny (Fig. 4B; monophyletic according to Bieler *et al.*, 2014; nonmonophyleyic according to Sharma *et al.*, 2013 and Combosch *et al.*, 2017). Shell microstructures of Solemyidae are variable, but their textural patterns were almost uniform among different species and different layers in the same specimens. As to the similarity of crystallographic textures among different layers, this might be related to the distribution of their shell layers associated with their unique mantle morphologies (Beedham & Owen, 1965; Taylor, Glover & Williams, 2008). While all species of Solemyida we analysed share granular crystals as the second- or third-order units in their microstructures, the textural pattern of *Huxleyia sulcata* (Manzanelloidea) did not resemble that of solemyids. Carter (1990) reported nacre-bearing Solemyidae from the Carboniferous. Thus, the microstructural composition of extant solemyids probably represents a secondary condition and the textural patterns of solemyids and manzanellids are not homologous.

Nuculanoidea: Since multiple nonmonophyletic (i.e. paraphyletic or polyphyletic) relationships were recognized for Nuculanoidea in a previous molecular study (Sharma *et al.*, 2013), we need to be careful when interpreting their character states in this superfamily. However, similar textural patterns were recognized in two *Yoldia* species. Both have outer homogeneous and inner fine CCL structures. Although the fine CCL of the two species slightly differs in the length of the acicular crystals composing the crossed-lamellar structure (see Sato & Sasaki, 2015), their textural patterns were type C. In addition, textural patterns of the shells of *Malletia takaii*, *Tindaria soyoae* and *Neilonella soyoae* were similar, despite their different shell microstructural components. These species are relatively close in the molecular phylogenetic tree of Sharma *et al.* (2013). Our results may indicate that they share the same mechanism of biomineralization. On the other hand, *N. tanseimaruae* and *Saccella gordonis*, both of which belong to Nuculanidae, do not share this crystallographic textural pattern. This demonstrates that shell microstructures and crystallographic textural patterns do not always coincide in the Nuculanoidea. This result could be explained by their controversial classification or by convergence due to habitat (e.g. water temperature). The nacreous structure is regarded as a plesiomorphy in the Protobranchia; nacre-bearing nuculanids have been reported from the Palaeozoic in the fossil record (Nevesskaya *et al.*, 1971; Carter, 1990; Vendrasco *et al.*, 2013; Sato & Sasaki, 2015). Therefore, the observed structures in each genus, such as the homogeneous structure, may have evolved independently from nacre.

Phylogenetic constraint of crystal orientation

Our data also showed that the orientation of crystals across whole shell layers changed in each superfamily, as summarized below.

Nuculoidea: This taxon had two to three textural patterns in an individual shell. Even the nacreous structures in the middle and inner layers clearly showed different patterns, except for two *Acila* species. The columnar nacreous structure in the middle layers of these species showed a ring-like pattern or a dyad symmetry clustering (types C and D) of the {102} pole maxima. Their inner layer consisted of sheet nacre with six maxima to nearly ring-like patterns (types C and E) for the {102} pole figure maxima. These results imply that either the *a*- and *b*-axes of nacre tablets become progressively disoriented as the nacreous layer thickens, or the crystallographic textures drastically change around the boundary of the middle and inner layers, where the myostracum is positioned. The latter possibility is more likely, because nacre tablets stack in different ways in the two layers (straight vertical stacking in columnar nacre and brickwall-like offset stacking in sheet nacreous structures; Sato & Sasaki, 2015). Chateigner *et al.* (2000) concluded that all bivalves had

poles. Asterisks indicate Manzanelloidea. **B.** Phylogenetic relationships of protobranchs and other bivalve taxa according to (i) Smith *et al.* (2011); (ii) Sharma *et al.* (2013); (iii) Bieler *et al.* (2014); (iv) Combosch *et al.* (2017). **C.** Correspondence between microstructures and their textural patterns. Abbreviations: cone CCL, cone complex crossed lamellar structure; CN, columnar nacreous structure; CP, composite prismatic structure; DCP, denticular composite prismatic structure; FA, foliated aragonite structure; fine CCL, fine complex crossed lamellar structure; FP, fibrous prismatic structure; Hom, homogeneous structure; IFP, irregular fibrous prismatic structure; INDCP, irregular nondenticular composite prismatic structure; NDCP, nondenticular composite prismatic structure; RESP, radially elongate prismatic structure; SN, sheet nacreous structure. In **A**: circle marks indicate presence of myostracum; triangles indicate that myostracum is obscure; crosses indicate absence of myostracum.

the same textural pattern (our type E) in their nacreous structures, while Frýda *et al.* (2010) claimed that bivalves nacre can be anything from ordered to unordered (our types C, D and E). These results conflict with each other, although both studies analysed the same species (*Pinna nobilis*, *Mytilus californianus* and *M. edulis*). One probable reason for this conflict is that these studies did not consider the existence of two nacreous layers separated by the myostracum. Chateigner *et al.* (2000) appear to have analysed the crystallographic texture of the nacreous structure near the inner shell surface for technical reasons, whereas Frýda *et al.* (2010) used shell fragments that were cut roughly in the middle of the nacreous shell layer. Thus, the former study may have analysed the inner nacreous layers, while the latter dealt with the middle layers. This hypothesis is reasonable, since the Neotrigonidae and Mytilidae are known to possess both columnar and sheet nacreous structures (Taylor *et al.*, 1969; Génio *et al.*, 2012). On the other hand, Checa & Rodríguez-Navarro (2005) confirmed that the textural pattern of the sheet nacreous structure of *P. nobilis* is almost uniform from the outer to the inner part. This explains why both studies (Chateigner *et al.*, 2000; Frýda *et al.*, 2010) showed the same result for *P. nobilis* (our type E).

Solemyida and Nuculanoidea: Unlike Nuculoidea, the crystallographic textures in the species we examined did not drastically differ from each other. Their textural patterns remained invariable from the outer to the inner layer; at most, they became slightly more ordered in the inward direction. This progressive crystal coorientation is probably due to competition between crystals, as demonstrated in calcitic prismatic structures of the outer layers in pteriomorphs (*Malleus regulus*, *Propeamussium sibogai* and *Ostrea puelchana*; Esteban-Delgado *et al.*, 2008). As mentioned above, the nacreous structure is likely to be a plesiomorphy in protobranchs. Moreover, each individual shell of Nuculoidea has two to three distinct textural patterns, in contrast to Solemyida and Nuculanoidea. Thus, the uniform crystallographic textures recognized in each of these two groups may imply that they have lost the intrinsic mechanism for regulating the calcium carbonate crystals.

Regulation of crystal growth by organic materials of the shell matrix has been reported in (1) nacre formation in pearl oysters (Rousseau *et al.*, 2009; Saruwatari *et al.*, 2009; Suzuki *et al.*, 2009) and (2) crystalline organization of the calcitic fibrous prismatic structure in *Mytilus galloprovincialis* (Checa *et al.*, 2014). In addition, homologues of shell-matrix proteins have been identified in closely related species (Sarashina *et al.*, 2006; Isowa *et al.*, 2012). Therefore, the above-mentioned homology of the crystallographic texture among protobranch superfamilies suggests that they share identical mechanisms of shell formation, including particular proteomic pools. Frýda, Bandel & Frýdová (2009) confirmed that the crystallographic texture of nacre in the Late Triassic gastropod *Wortheniella coralliophila* is similar to that in modern vetigastropods and suggested that the molecular and physical mechanisms of nacre formation in gastropods have remained unchanged since that time. In the future, further SEM and XRD studies of shell microstructures will provide better knowledge on the evolution of microstructures, as well as on the physical and molecular mechanisms of biomineralization.

CONCLUSIONS

Our analysis revealed interspecific unity and homology of the crystallographic textures of shell microstructures in Protobranchia, which is regarded as the most basal group of the Bivalvia.

(1) Two to three distinct textural patterns were recognized in nuculoidean shells. The categorized types of crystallographic textures in their outer layers are consistent with their phylogenetic relationships. Re-evaluation of the microstructures in the outer layer based both on SEM observations and XRD analysis will provide a reliable basis for the identification of extant and fossil nuculids. The two types of nacreous structures, columnar and sheet in the middle and inner layers, respectively, can be distinguished by their textural patterns in most species.

(2) In Solemyida, the crystallographic textures are uniform, despite the diversity in their shell microstructures.

(3) In Nuculanoidea, morphologically similar microstructures do not always have the same crystallographic textures. However, in most cases, closely related species share similar textural patterns regardless of differences in shell microstructure. Thus, their crystallographic textures seem to be constrained phylogenetically.

(4) The crystallographic textures in Solemyida and Nuculanoidea do not change drastically from the outer to the inner layers. Since molecular phylogenetic and palaeontological data suggest that the Solemyida and Nuculanoidea are relatively derived taxa (in contrast to the Nuculoidea), the crystallography of their microstructures can be regarded as apomorphic within the Protobranchia.

SUPPLEMENTARY MATERIAL

Supplementary material is available at *Journal of Molluscan Studies* online.

ACKNOWLEDGEMENTS

We are very grateful to Prof. Kazuyoshi Endo, Dr Takanobu Tsuihiji, Dr Toshihiro Kogure and Dr Yasunori Kano (University of Tokyo, UT) for their valuable comments and suggestions. We thank also Dr Koji Seike (UT) for donating specimens. We were able to participate in research surveys and collecte deep-sea protobranchs through the courtesy of Prof. Koji Inoue (UT) and Dr Toshiro Saruwatari (UT). We also thank the crew of the R/V *Tansei-Maru* and R/V *Sinsei-Maru* (Japan Agency for Marine-Earth Science and Technology), R/V *Nagasaki-Maru* (Nagasaki University) and the staff of Misaki Marine Biological Station (UT), for their kind assistance in collecting material. Our XRD analyses were technically assisted by Dr Hyuma Masu (Chiba University) and José Romero (Universidad de Granada). This research was supported by Grants-in-Aid for Scientific Research (24654167, 26291077) from the Japan Society for the Promotion of Science and by the research projects CGL2013-48247-P and CGL2015-64683-P [Spanish Ministry of Economy and Competitiveness (Ministerio Español de Economía, Industria y Competitividad)]. We thank two anonymous referees for their constructive comments.

REFERENCES

ALMAGRO, I., DRZYMAŁA, P., BERENT, K., SAINZ-DÍAZ, C.I., WILLINGER, M.G., BONARSKI, J. & CHECA, A.G. 2016. New crystallographic relationships in biogenic aragonite: the crossed-lamellar microstructures of mollusks. *Crystal Growth & Design*, **16**: 2083–2093.

ÁLVAREZ-LLORET, P., RODRIGUEZ-NAVARRO, A.B. & CHECA, A.G. 2008. Evolution of the microstructure and crystallographic orientation during shell growth in *Psilunio littoralis* and *Nautilus belauensis*. *Mineralogical Magazine*, **72**: 163–167.

BEEDHAM, G.E. & OWEN, G. 1965. The mantle and shell of *Solemya parkinsoni* (Protobranchia: Bivalvia). *Proceedings of the Zoological Society of London*, **145**: 405–430.

BIELER, R., MIKKELSEN, P.M., COLLINS, T.M., GLOVER, E.A., GONZÁLEZ, V.L., GRAF, D.L., HARPER, E.M., HEALY, J., KAWAUCHI, G.Y., SHARMA, P.P., STAUBACH, S., STRONG, E.E., TAYLOR, J.D., TËMKIN, I., ZARDUS, J.D., CLARK, S.,

GUZMÁN, A., MCINTYRE, E., SHARP, P. & GIRIBET, G. 2014. Investigating the Bivalve Tree of Life—an exemplar-based approach combining molecular and novel morphological characters. *Invertebrate Systematics*, **28**: 32–115.

BØGGILD, O.B. 1930. The shell structure of the mollusks. *Det Kongelige Danske Videnskabernes Selskabs Skrifter, Naturvidenskabelig og Mathematisk, Afdeling, Ser. 9*, **2**: 231–326.

BOUCHET, P., ROCROI, J.-P., BIELER, R., CARTER, J.G. & COAN, E.V. 2010. Nomenclator of bivalve families with a classification of bivalve families. *Malacologia*, **52**: 1–184.

CARTER, J.G. 1990. *Skeletal biomineralization: patterns, processes and evolutionary trends*, Vols 1, 2. Van Nostrand Reinhold, New York.

CARTER, J.G. 2001. Shell and ligament microstructure of selected Silurian and Recent palaeotaxodonts (Mollusca: Bivalvia). *American Malacological Bulletin*, **16**: 217–238.

CARTER, J.G., HARRIES, P., MALCHUS, N., SARTORI, A., ANDERSON, L., BIELER, R., BOGAN, A., COAN, E., COPE, J., CRAGG, S., GARCIA-MARCH, J., HYLLEBERG, J., KELLEY, P., KLEEMANN, K., KRIZ, J., MCROBERTS, C., MIKKELSEN, P., POJETA, J.JR., SKELTON, P.W., TEMKIN, I., YANCEY, T. & ZIERITZ, A. 2012. Illustrated glossary of the Bivalvia. *Treatise on Invertebrate Paleontology*, Part N, revised, Vol. 1. *Treatise Online*, **48**: 1–209.

CHATEIGNER, D., HEDEGAARD, C. & WENK, H.-R. 2000. Mollusc shell microstructures and crystallographic textures. *Journal of Structural Geology*, **22**: 1723–1735.

CHECA, A.G., PINA, C.M., OSUNA-MASCARÓ, A.J., RODRÍGUEZ-NAVARRO, A.B. & HARPER, E.M. 2014. Crystalline organization of the fibrous prismatic calcitic layer of the Mediterranean mussel *Mytilus galloprovincialis*. *European Journal of Mineralogy*, **26**: 495–505.

CHECA, A.G. & RODRÍGUEZ-NAVARRO, A.B. 2005. Self-organisation of nacre in the shells of Pterioida (Bivalvia: Mollusca). *Biomaterials*, **26**: 1071–1079.

COAN, E.V. & VALENTICH-SCOTT, P. 2012. *Bivalve seashells of tropical West America.* Santa Barbara Museum of Natural History, Santa Barbara.

COMBOSCH, D.J., COLLINS, T.M., GLOVER, E.A., GRAF, D.L., HARPER, E.M., HEALY, J.M., KAWAUCHI, G.Y., LEMER, S., MCINTYRE, E., STRONG, E.E., TAYLOR, J.D., ZARDUS, J.D., MIKKELSEN, P.M., GIRIBET, G. & BIELER, R. 2017. A family-level tree of life for bivalves based on a Sanger-sequencing approach. *Molecular Phylogenetics and Evolution*, **107**: 191–208.

ESTEBAN-DELGADO, F.J., HARPER, E.M., CHECA, A.G. & RODRÍGUEZ-NAVARRO, A.B. 2008. Origin and expansion of foliated microstructure in pteriomorph bivalves. *Biological Bulletin*, **214**: 153–165.

FENG, W.M. & SUN, W.G. 2003. Phosphate replicated and replaced microstructure of molluscan shells from the earliest Cambrian of China. *Acta Palaeontologica Polonica*, **48**: 21–30.

FRÝDA, J., BANDEL, K. & FRÝDOVÁ, B. 2009. Crystallographic texture of Late Triassic gastropod nacre: evidence of long-term stability of the mechanism controlling its formation. *Bulletin of Geosciences*, **84**: 745–754.

FRÝDA, J., KLICNAROVÁ, K., FRÝDOVÁ, B. & MERGL, M. 2010. Variability in the crystallographic texture of bivalve nacre. *Bulletin of Geosciences*, **85**: 645–662.

FUCHIGAMI, T. & SASAKI, T. 2005. The shell structure of the Recent Patellogastropoda (Mollusca: Gastropoda). *Paleontological Research*, **9**: 143–168.

GÉNIO, L., KIEL, S., CUNHA, M.R., GRAHAME, J. & LITTLE, C.T. S. 2012. Shell microstructures of mussels (Bivalvia: Mytilidae: Bathymodiolinae) from deep-sea chemosynthetic sites: do they have a phylogenetic significance? *Deep Sea Research Part I: Oceanographic Research Papers*, **64**: 86–103.

HAHN, S., GRIESSHABER, E., SCHMAHL, W.W., NEUSER, R.D., RITTER, A.C., HOFFMANN, R., BUHL, D., NIEDERMAYR, A., GESKE, A. & IMMENHAUSER, A. 2014. Exploring aberrant bivalve shell ultrastructure and geochemistry as proxies for past sea water acidification. *Sedimentology*, **61**: 1625–1658.

HEDEGAARD, C., LINDBERG, D.R. & BANDEL, K. 1997. Shell microstructure of a Triassic patellogastropod limpet. *Lethaia*, **30**: 331–335.

HUBER, M. 2010. *Compendium of bivalves*. Conchbooks, Hackenheim.

ISOWA, Y., SARASHINA, I., SETIAMARGA, D.H.E. & ENDO, K. 2012. A comparative study of the shell matrix protein aspein in pterioid bivalves. *Journal of Molecular Evolution*, **75**: 11–18.

KOUCHINSKY, A. 2000. Shell microstructures in Early Cambrian molluscs. *Acta Palaeontologica Polonica*, **45**: 119–150.

MACCLINTOCK, C. 1967. Shell structure of patelloid and bellerophontoid gastropods (Mollusca). *Bulletin of the Peabody Museum of Natural History, Yale University*, **22**: 1–140.

NEVESSKAYA, L.A., SCARLATO, O.A., STAROBOGATOV, Y.I. & EBERZIN, A.G. 1971. New ideas on bivalve systematics. *Paleontological Journal*, **5**: 141–155.

OLSON, I.C. & GILBERT, P.U.P.A. 2012a. Aragonite crystal orientation in mollusk shell nacre may depend on temperature. The angle spread of crystalline aragonite tablets records the water temperature at which nacre was deposited by *Pinctada margaritifera*. *Faraday Discussions*, **159**: 421–432.

OLSON, I.C., KOZDON, R., VALLEY, J.W. & GILBERT, P.U.P.A. 2012b. Mollusk shell nacre ultrastructure correlates with environmental temperature and pressure. *Journal of the American Chemical Society*, **134**: 7351–7358.

RODRIGUEZ-NAVARRO, A.B. 2006. XRD2DScan: new software for polycrystalline materials characterization using two-dimensional X-ray diffraction. *Journal of Applied Crystallography*, **39**: 905–909.

ROUSSEAU, M., MEIBOM, A., GÈZE, M., BOURRAT, X., ANGELLIER, M. & LOPEZ, E. 2009. Dynamics of sheet nacre formation in bivalves. *Journal of Structural Biology*, **165**: 190–195.

SARASHINA, I., YAMAGUCHI, H., HAGA, T., IIJIMA, M., CHIBA, S. & ENDO, K. 2006. Molecular evolution and functionally important structures of molluscan dermatopontin: implications for the origins of molluscan shell matrix proteins. *Journal of Molecular Evolution*, **62**: 307–318.

SARUWATARI, K., MATSUI, T., MUKAI, H., NAGASAWA, H. & KOGURE, T. 2009. Nucleation and growth of aragonite crystals at the growth front of nacres in pearl oyster, *Pinctada fucata*. *Biomaterials*, **30**: 3028–3034.

SATO, K., NAKASHIMA, R., MAJIMA, R., WATANABE, H. & SASAKI, T. 2013. Shell microstructures of five Recent solemyids from Japan (Mollusca: Bivalvia). *Paleontological Research*, **17**: 69–90.

SATO, K. & SASAKI, T. 2015. Shell microstructure of Protobranchia (Mollusca: Bivalvia): diversity, new microstructures and systematic implications. *Malacologia*, **59**: 45–103.

SCHNEIDER, J.A. & CARTER, J.G. 2001. Evolution and phylogenetic significance of Cardioidean shell microstructure (Mollusca, Bivalvia). *Journal of Paleontology*, **75**: 607–643.

SHARMA, P.P., ZARDUS, J.D., BOYLE, E.E., GONZÁLEZ, V.L., JENNINGS, R.M., MCINTYRE, E., WHEELER, W.C., ETTER, R. J. & GIRIBET, G. 2013. Into the deep: a phylogenetic approach to the bivalve subclass Protobranchia. *Molecular Phylogenetetics and Evolution*, **69**: 188–204.

SMITH, S.A., WILSON, N.G., GOETZ, F.E., FEEHERY, C., ANDRADE, S.C.S., ROUSE, G.W., GIRIBET, G. & DUNN, C.W. 2011. Resolving the evolutionary relationship of molluscs with phylogenomic tools. *Nature*, **480**: 364–367.

SPANN, N., HARPER, E.M. & ALDRIDGE, D.C. 2010. The unusual mineral vaterite in shells of the freshwater bivalve *Corbicula fluminea* from the UK. *Die Naturwissenschaften*, **97**: 743–751.

SUZUKI, M., SARUWATARI, K., KOGURE, T., YAMAMOTO, Y., NISHIMURA, T., KATO, T. & NAGASAWA, H. 2009. An acidic matrix protein, Pif, is a key macromolecule for nacre formation. *Science*, **325**: 1388–1390.

TAYLOR, J.D., KENNEDY, W.J. & HALL, A. 1969. The shell structure and mineralogy of the Bivalvia. Introduction. Nuculacea–Trigonacea. *Bulletin of the British Museum (Natural History)*, **3**: 1–125.

TAYLOR, J.D., KENNEDY, W.J. & HALL, A. 1973. The shell structure and mineralogy of the Bivalvia II. Lucinacea–Clavagellacea, conclusions. *Bulletin of the British Museum (Natural History)*, **22**: 225–294.

TAYLOR, J.D. & REID, D.G. 1990. Shell microstructure and mineralogy of the Littorinidae: ecological and evolutionary significance. *Hydrobiologia*, **193**: 199–215.

TAYLOR, J.D., GLOVER, E.A. & WILLIAMS, A.T. 2008. Ancient chemosynthetic bivalves: systematics of Solemyidae from eastern and southern Australia (Mollusca: Bivalvia). *Memoirs of the Queensland Museum*, **54**: 75–104.

UOZUMI, S. & SUZUKI, S. 1981. The evolution of shell structures in the Bivalvia. In: *Study of molluscan paleobiology* (T. Habe & M. Omori, eds), pp. 63–77. Niigata University, Niigata.

VENDRASCO, M.J., CHECA, A., HEIMBROCK, W. & BAUMANN, S. 2013. Nacre in molluscs from the Ordovician of the Midwestern United States. *Geosciences*, **3**: 1–29.

VENDRASCO, M.J., CHECA, A.G. & KOUCHINSKY, A.V. 2011. Shell microstructure of the early bivalve *Pojetaia* and the independent origin of nacre within the Mollusca. *Palaeontology*, **54**: 825–850.

ZARDUS, J.D. 2002. Protobranch bivalves. *Advances in Marine Biology*, **42**: 1–65.

WADA, K. 1972. Nucleation and growth of aragonite crystals in the nacre of some bivalve molluscs. *Biomineralization*, **6**: 141–159.

WORMS. 2016. *World Register of Marine Species*. Available from http://www.marine species.org. at VLIZ. Accessed 27 September 2016.